Imaging a two-dimensional electron system with a scanning charged probe

Subhasish Chakraborty, I. J. Maasilta,* and S. H. Tessmer
Department of Physics and Astronomy, Michigan State University, East Lansing, Michigan 48824

M. R. Melloch
Department of Electrical Engineering, Purdue University, West Lafayette, Indiana 47907
(Received 3 October 2003; published 20 February 2004)

We introduce a new and conceptually simple scanning probe method to resolve potential fluctuations within a GaAs two-dimensional electron system (2DES). The method employs a charged metal tip to deplete locally the 2DES. The depletion is detected as a reduction in capacitance, measured using a cryogenic transistor attached directly to the tip. The resulting images exhibit contrast arising from variations in the disorder potential. We find the disorder forms random patterns dominated by length scales greater than 0.5 μm. This surprising result is not consistent with present theories, which predict that no preferred wavelengths should be present on the micron scale.

DOI: 10.1103/PhysRevB.69.073308 PACS number(s): 73.40.−c, 73.23.−b

The integer and fractional quantum Hall effects in two-dimensional electron systems (2DES) are among the most remarkable phenomena to be discovered in condensed matter physics in the past two decades.[1,2] Disorder in these systems gives rise to localized states that play a major role—hence a complete description of sample disorder is crucial.[3,4] In GaAs systems, the 2DES typically resides 20–100 nm below a layer of ionized Si donors. The main source of disorder is believed to be the random distribution of these charged ions, resulting in a potential in the 2D layer V_{disorder} that contains random fluctuations. In contrast to conventional transport measurements, which give the spatially-averaged 2DES disorder, scanning probe techniques sensitive to local electric fields offer the possibility to directly measure nanometer-scale properties of the 2DES. These techniques include scanning single-electron transistor microscopy,[5–7] charged-probe force microscopy,[8–10] and subsurface charge accumulation (SCA) imaging.[11–13]

Here we report a new cryogenic scanning probe method, based on SCA imaging, capable of resolving potential fluctuations within a GaAs system. Similar to charged-probe force microscopy, a voltage V_{tip} is applied to the tip to locally perturb the 2D layer. Conceptually, our method is very simple. A negative V_{tip} pushes away electrons in the 2D layer below the tip's apex. The reduced density results in a reduction of the tip-2DES capacitance, which we measure using a cryogenic transistor attached directly to the tip. Because the disorder potential also contributes to the local depletion, by scanning the charged probe we can map out variations in V_{disorder}. We find the disorder potential forms random patterns with surprisingly long characteristic length scales greater than 500 nm. This result agrees with a recent study performed Finkelstein and co-workers, which utilized a more complex few-electron-bubble method to achieve contrast.[14]

The sample used for these measurements was an $Al_{0.3}Ga_{0.7}As/GaAs(001)$ wafer grown by molecular beam epitaxy (MBE), shown schematically in Fig. 1(a). The 2DES is located at a distance of $d_1 = 60$ nm below the exposed surface, and a distance $d_2 = 40$ nm above a degenerately doped (10^{18} cm^{-3}) GaAs substrate (3D metal). An AlGaAs tunneling barrier separates the 2D and 3D layers. The average electron density in the 2DES is 6×10^{11} cm^{-2}, the low-temperature transport mobility is $\sim10^5$ cm^2/Vs, and the characteristic 3D–2D tunneling rate is approximately 200 kHz. Figure 1(b) schematically shows the method, which works as follows: An ac excitation voltage V_{exc} applied between the 3D substrate and a sharp metal tip locally induces charge to tunnel back and forth between the 3D and 2D layers. A Schottky barrier blocks the charge from tunneling directly onto the tip. The measured signal is the resulting ac image charge q on the tip electrode, which is proportional to the number of ac electric field lines terminating on it. For the measurements shown here, $V_{\text{exc}} = 8$ mV rms at a frequency 20 kHz. We find this excitation amplitude to be sufficiently small to ensure that the system is in linear response. Moreover, because the excitation frequency is small compared to the zero-field tunneling rate, the 2DES has sufficient time to charge fully during each cycle and the charging is approximately in-phase with the excitation. Hence the measurement is essentially a local probe of the tip-2DES capacitance: C

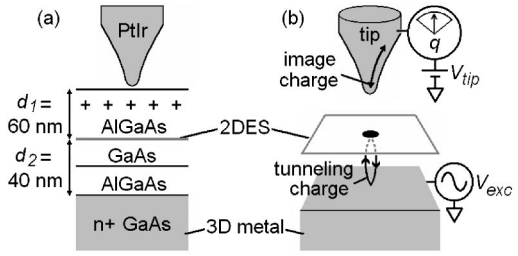

FIG. 1. (a) Schematic of heterostructure sample. The 2D layer forms in the potential well at the GaAs/AlGaAs interface from electrons provided by silicon dopants (+'s). Randomness in the dopant distribution is believed to be the main source of disorder. An AlGaAs tunneling barrier separates the 2DES from the 3D substrate. (b) Schematic of measurement technique. Charge is induced locally to tunnel from a three-dimensional substrate into the two-dimensional layer by applying an ac excitation voltage V_{exc} between the tip and substrate. This results in ac image charge q on the tip which is proportial to the capacitance $C = q/V_{\text{exc}}$.

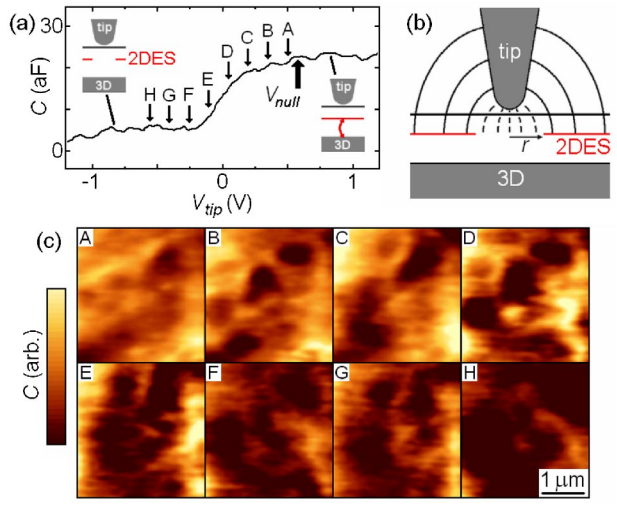

FIG. 2. (Color online) (a) Representative fixed-tip measurement of the capacitance C as a function of dc tip voltage V_{tip}. As negative voltages tends to deplete the 2D layer, the signal shifts from the relatively high tip-to-2D capacitance at positive V_{tip} to the lower tip-to-3D capacitance at negative V_{tip}. The large arrow indicates the effective zero potential V_{null}. The data were acquired at 0.3 K. (b) An intuitive picture used to estimate the spatial resolution of the technique. The 2DES is assumed to be completely depleted below the apex of the tip out to a radius r. This results in ''missing'' field lines compared to the accumulated case, shown as dashes. Therefore, in depletion less image charge is induced on the tip. (c) A series of 3×3 μm capacitance images acquired at tip voltages spanning a range of $V_{\mathrm{tip}}=0.50$ V$--0.55$ V as indicated in (a). The displayed images are filtered to remove nanometer scale scatter. The images were acquired at 1.5 K.

$=q/V_{\mathrm{exc}}$. Both the geometrical capacitance and 2DES thermodynamic density of states contribute to C.[15,16] The typical units are 10^{-18} C/V$=1$ aF.

We position the tip to within a few nanometers of the sample surface using an innovative and highly stable scanning probe microscope.[17] The image charge signal is detected using a circuit constructed from a low-input-capacitance high-electron-mobility transistor (noise level 0.01 electrons/$\sqrt{}$Hz). Most of the signal ($\sim$99.8%) corresponds to electric field emanating from areas macroscopically far from the location under the probe.[16] We subtract away this background signal using a bridge circuit. To acquire images, the tip is scanned laterally across the surface without the use of feedback. Cryogenic temperatures were achieved using a helium-3 cryostat, either by direct immersion in liquid helium-3 at 0.3 K, or by using the helium-3 as an exchange gas while regulating the temperature with a thermally-coupled helium-4 pot.

Figure 2(a) shows a representative measurement of the capacitance as a function of tip voltage, performed with the tip held at a fixed location (i.e., not scanned). The large arrow marks the nulling voltage $V_{\mathrm{tip}}=V_{\mathrm{null}}=0.6$ V, measured using the Kelvin probe technique.[11] This is the effective zero point where the applied voltage compensates for the tip–sample contact potential.[5] In other words, at V_{null} there is no dc electric field between the tip and sample. As V_{tip} becomes negative with respect to V_{null}, the tip begins to deplete the 2DES and the capacitance drops. We see that near $V_{\mathrm{tip}}=-0.3$ V the capacitance again levels off, forming a characteristic steplike curve.[18] This indicates that at -0.3 V the 2DES below the apex of the tip is nearly completely depleted. The magnitude of the step is $\Delta C=20$ aF.

Figure 2(b) gives an intuitive picture for the measurement. We assume the 2DES is completely depleted below the apex of the tip out to an effective radius r. This forms a hole into which charge can no longer tunnel in response to the ac excitation. Hence ac electric field lines near the apex of the tip are missing as indicated by the dashes (to be replaced by a set of fewer lines emanating directly from the 3D substrate). Therefore less image charge is induced on the tip compared to the accumulated case, and the capacitance is reduced. The radius of the depleted area is a key parameter as it determines the spatial resolution of the scanning measurements. Using a simple parallel plate model we can estimate roughly r from the magnitude of ΔC. If we assume that both the tip-to-2DES and the tip-to-3D substrate capacitances can be approximated as parallel plates of area πr^2, the capacitance step can be expressed as $\Delta C=20$ aF $=(\pi r^2)\kappa\varepsilon_0[1/d_1-1/(d_1+d_2)]$, where $\kappa=12.5$ is the GaAs dielectric constant. This estimate gives approximately $r=90$ nm, a value somewhat larger than the 50 nm radius of curvature of the chemically etched PtIr tip.[19] This value compares well to a detailed numerical calculation we have performed for this system, which predicts a spatial resolution length of 92 nm.[20] Moreover a direct comparison of the calculation to the sharpest features discerned in scanning measurements (employing the same tip and sample as the images presented below) shows reasonable agreement.[20]

Figure 2(c) shows a series of capacitance images labeled A–H, acquired at 1.5 K over a 3×3 μm area by scanning the tip while depleting the 2DES. The tip voltage is decremented by 0.15 V for each displayed image, indicated in Fig. 2(a) by the small arrows. The figure represents a subset of the total data set, which consisted of 34 images acquired in decrement of 0.075 V over a voltage range of $V_{\mathrm{tip}}=0.5$ V$--0.7$ V. The time span to acquire the data was 12 h. We observed only small drifts in tip–sample separation $\sim$1 nm over this long period of time, a testament to the high degree of mechanical and thermal stability achieved by the system. In the figure, brighter shades correspond to greater C. Hence for image A, which was acquired just below the nulling voltage at $V_{\mathrm{tip}}=0.5$ V, the relative capacitance is high. For each subsequent image, the 2DES density is further reduced and C falls off accordingly. As expected, the entire area becomes relatively dark near $V_{\mathrm{tip}}=-0.25$ V.

To extract the detailed structure of the disorder potential from these images, we must consider that the geometrical capacitance will contribute to C, in addition to the 2DES thermodynamic density of states. In other words, we interpret the features in Fig. 2(c) as a convolution of surface topography and disorder potential variations. To isolate approximately the disorder potential contribution, for each unfiltered image we subtracted a scaled reference image that represents the topographical contribution. We used image A

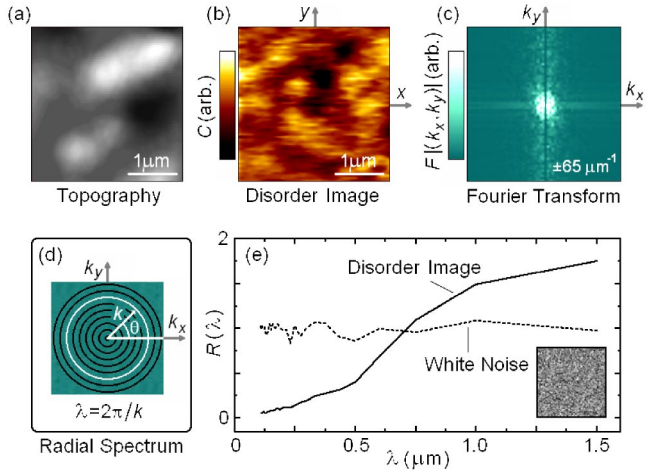

FIG. 3. (Color online) (a) A 3×3 μm scanning tunneling microscopy image of surface topography acquired at room temperature. The elongated moundlike growth features are typical for GaAs (001) and are approximately 5 nm tall. (b) Capacitance image for $V_{\text{tip}}=0.350$ V, processed to remove the topographical contribution to the signal. The image represents variations in the disorder potential and shows intriguing droplet features of size ~0.5 μm. (c) Fourier transform of (b) over a range of ±65 μm^{-1}. The minimum along the k_y axis ($k_x=0$) is an artifact of the processing. (d) Schematic of the radial spectrum calculation used to identify the dominant wavelengths. $R(\lambda)$ is found by integrating the transform image along a series of circles of radius $k=2\pi/\lambda$. (e) Radial spectrum of (b) compared to the spectrum of a numerically generated 3×3 μm random "white noise" image (inset). The curves are normalized to have an average value of 1.0.

as the reference since it has the minimal depletion, hence we expect that the contrast arises mostly from topography. Moreover, the diagonal ridges present in the image are qualitatively similar to the surface growth features observed on the sample,[21] an example of which is shown in Fig. 3(a). After subtracting image A, as a last step we reduced small drift effects by subtracting an offset and slope from each line of the processed image. No further processing or filtering was performed.

We find that the processed images in the range of $V_{\text{tip}}=0.425-0.275$ V all showed very similar structure, as shown in Fig. 3(b) which exhibits the $V_{\text{tip}}=0.350$ V data [corresponding to image B of Fig. 2(c)]. The structure appears to consist mostly of randomly distributed micron-scale droplets. These features are qualitatively different from both image A and the typical topographical surface features, shown in Fig. 3(a). In principle, it is possible that the features arise from topographic structure at the 3D-tunneling barrier interface, 100 nm below the surface. However, this is unlikely because this interface topography should closely mirror the surface topography.[21] Hence we assert that Fig. 3(b) represents a direct map of V_{disorder}. We find that at tip voltages lower that 0.275 V, the pattern begins to become distorted and many of the droplet features disappear; this effect can already be seen in the unprocessed images of Fig. 2(c).

The observation that the features persist over a tip voltage range of 0.425–0.275 V, or $\Delta V_{\text{tip}}=150$ mV, allows us to estimate roughly the magnitude of the disorder potential fluctuations in the 2D layer. To translate V_{tip} variations into V_{disorder} variations, we consider two capacitors in series: $C_{\text{tip-2D}}$ and $C_{\text{2D-3D}}$. We can then write $\Delta V_{\text{disorder}}=\Delta V_{\text{tip}}\,[C_{\text{tip-2D}}/(C_{\text{tip-2D}}+C_{\text{2D-3D}})]$. From Ref. 20 we find that the capacitance per unit area below the apex of the tip is $C_{\text{tip-2D}}\approx1\times10^{-4}$ F/m^2, whereas the 2D-to-3D capacitance per unit area is $C_{\text{2D-3D}}=\kappa\varepsilon_0/d_2=2.5\times10^{-3}$ F/m^2. We then find $\Delta V_{\text{disorder}}\sim5$ mV, roughly a factor of 2 larger than the estimated value in Ref. 14.

To the eye, Fig. 3(b) appears to be dominated by droplet-like features of size ~0.5 μm. To more quantitatively extract the length scales present in the processed images, we applied a standard approach based on the 2D Fourier transforms: $F(k_x,k_y)=\mathcal{F}[C(x,y)]$, where k_x and k_y are the wave vector coordinates. No additional filtering or processing was performed on the data prior to taking the Fourier transforms. Figure 3(c) shows the Fourier transform of Fig. 3(b). The minimum along the k_y axis is an artifact resulting from subtracting the offset and slope from each line of the direct image. We then calculate the radial spectrum R by integrating the Fourier transform along a set of circles of radius k: $R(\lambda)=R(k=2\pi/\lambda)=\int|F(k\cos\theta,k\sin\theta)|d\theta$, as shown schematically in Fig. 3(d).

Figure 3(e) shows the radial spectrum of Fig. 3(b). We see that relatively long wavelengths greater than 0.5 μm dominate the spectrum, confirming the expectation. We find no evidence that the depleting voltage itself plays a role in forming the micron scale structure. For example, we find nearly identical structure for the $V_{\text{tip}}=0.425$ V and $V_{\text{tip}}=0.350$ V data—for both the direct images and radial spectra. For comparison, Fig. 3(e) also shows the spectrum from a numerically generated "white noise" image in which all wavelengths contribute approximately equally.

The observed micron-size disorder length scale is surprising in light of the conventional picture that the MBE growth results in an entirely random spatial distribution of Si donors.[22–26] The charge distribution may change as a result of electron migration between the donors. However, this effect is expected to suppress (not enhance) long-range fluctuations. The interdonor distance in our sample is approximately 10 nm, calculated from the Si density of 10^{18} cm^{-3}, bulk doped over an AlGaAs thickness of 10 nm. The other key length scale is the donor layer-2DES distance which is expected to set the minimum length for fluctuations in V_{disorder}. For our sample this is 20 nm, smaller than our spatial resolution of 90 nm. Hence the disorder potential should appear completely random to our 90 nm experimental resolution, giving an appearance similar to the white noise image shown as an inset in Fig. 3(e).

Our observations agree approximately with a recent study performed by Finkelstein and co-workers[14] for the length scale of V_{disorder} fluctuations. That study probed a sample grown in a different MBE machine, using the few-electron-bubble method to resolve the disorder potential. The technique utilizes the formation of a quantum dot below the apex of the tip while a magnetic field brings the 2DES to near integer Landau level filling; the addition spectrum of the dot

is sensitive to the disorder potential fluctuations. In contrast, our method is conceptually much simpler and requires no applied magnetic field.

In summary, we have developed a new low-temperature scanning probe method sensitive to potential fluctuations within a GaAs two dimensional electron system. The method simply employs a charged probe to deplete locally the 2D layer, reducing the measured capacitance between the probe and the layer. By scanning the probe we can image variations in the disorder potential, which also contributes to the local depletion. We find the disorder potential forms random patterns with dominant length scales greater than 0.5 μm. This result is surprising as it is inconsistent with present theories, which predict that no characteristic wavelengths should be present in the system larger than our experimental spatial resolution of 90 nm.

We thank M. I. Dykman, A. L. Efros, and A. H. MacDonald for helpful discussions and comments. This work was supported by the National Science Foundation Grant Nos. DMR00-75230 and DMR03-05461. S.H.T. acknowledges support of the Alfred P. Sloan Foundation.

*Current address: Department of Physics, P.O. Box 35, FIN-40014, University of Jyväskylä, Finland.

[1] K. von Klitzing, G. Dorda, and M. Pepper, Phys. Rev. Lett. **45**, 494 (1980).
[2] D. C. Tsui, H. L. Stormer, and A. C. Gossard, Phys. Rev. Lett. **48**, 1559 (1982).
[3] *The Quantum Hall Effect*, 2nd ed., edited by R. E. Prange and S. M. Girvin (Springer-Verlag, New York, 1987).
[4] *Perspectives in Quantum Hall Effects*, edited by S. Das Sarma and A. Pinczuk (Wiley, New York, 1997).
[5] M. J. Yoo, T. A. Fulton, H. F. Hess, R. L. Willett, L. N. Dunkleberger, R. J. Chichester, L. N. Pfeiffer, and K. W. West, Science **276**, 579 (1997).
[6] A. Yacoby, H. F. Hess, T. A. Fulton, L. N. Pfeiffer, and K. W. West, Solid State Commun. **111**, 1 (1999).
[7] N. B. Zhitenev, T. A. Fulton, A. Yacoby, H. F. Hess, L. N. Pfeiffer, and K. W. West, Nature (London) **404**, 473 (2000).
[8] M. A. Eriksson, R. G. Beck, M. Topinka, and J. A. Katine, Appl. Phys. Lett. **69**, 671 (1996).
[9] M. A. Topinka, B. J. LeRoy, S. E. J. Shaw, E. J. Heller, R. M. Westervelt, K. D. Maranowski, and A. C. Gossard, Science **289**, 2323 (2000).
[10] M. A. Topinka, B. J. LeRoy, R. M. Westervelt, S. E. J. Shaw, R. Fleischmann, E. J. Heller, K. D. Maranowski, and A. C. Gossard, Nature (London) **410**, 183 (2001).
[11] S. H. Tessmer, P. I. Glicofridis, R. C. Ashoori, L. S. Levitov, and M. R. Melloch, Nature (London) **392**, 51 (1998).
[12] G. Finkelstein, P. I. Glicofridis, S. H. Tessmer, R. C. Ashoori, and M. R. Melloch, Phys. Rev. B **61**, R16 323 (2000).
[13] I. J. Maasilta, Subhasish Chakraborty, I. Kuljanishvili, S. H. Tessmer, and M. R. Melloch, Phys. Rev. B **68**, 205328 (2003).
[14] G. Finkelstein, P. I. Glicofridis, R. C. Ashoori, and M. Shayegan, Science **289**, 90 (2000).
[15] F. Stern, internal IBM technical report, 1972 (unpublished).
[16] S. H. Tessmer, G. Finkelstein, P. I. Glicofridis, and R. C. Ashoori, Phys. Rev. B **66**, 125308 (2002).
[17] S. Urazhdin, I. J. Maasilta, S. Chakraborty, I. Moraru, and S. H. Tessmer, Rev. Sci. Instrum. **71**, 4170 (2000).
[18] See, for example, R. C. Ashoori, H. L. Stormer, J. S. Weiner, L. N. Pfeiffer, S. J. Pearton, K. W. Baldwin, and K. W. West, Phys. Rev. Lett. **68**, 3088 (1992).
[19] Materials Analytical Services, 616 Hutton Street, Suite 101, Raleigh, NC 27606.
[20] I. Kuljanishvili, Subhasish Chakraborty, I. J. Maasilta, and S. H. Tessmer, cond-mat/0309667 (preprint).
[21] A. Ballestad, B. J. Ruck, M. Adamcyk, T. Pinnington, and T. Tiedje, Phys. Rev. Lett. **86**, 2377 (2001).
[22] A. L. Efros, Solid State Commun. **65**, 1281 (1988).
[23] A. L. Efros, Phys. Rev. B **60**, 13343 (1999).
[24] N. R. Cooper and J. T. Chalker, Phys. Rev. B **48**, 4530 (1993).
[25] W. Walukiewicz, H. E. Ruda, J. Lagowski, and H. C. Gatos, Phys. Rev. B **30**, 4571 (1984).
[26] S. Munnix, R. K. Bauer, D. Bimberg, J. S. Harris, R. Kohrbruck, E. C. Larkins, C. Maierhofer, D. E. Mars, and J. N. Miller, J. Vac. Sci. Technol. B **7**, 704 (1989).